Scientific Research Publishing

Characterization of Pan-African Aquifer Layers by the Least Squares Inversion Method Applied on Geoelectric Data

Kana T. Idriss[1], Serge H. Pokam Kengni[1,2], Ndikum Eric Ndoh[1,3*], Blaise P. Gounou Pokam[1], Charles T. Tabod[1,2]

[1]Department of Physics, Faculty of Science, University of Yaounde I, Yaounde, Cameroon
[2]Department of Physics, Faculty of Science, University of Bamenda, Bamenda, Cameroon
[3]Department of Physics, HTTC Bambili, University of Bamenda, Bamenda, Cameroon
Email: *ndikumeric@yahoo.com

Abstract

Geoelectric data obtained from forty (40) vertical electrical soundings collected with a Schlumberger device in the Adamawa plateau region, also known as the Cameroon water tower, have been treated by the least-squares inversion method. In order to study the nature and thickness of the aquifer and the necessary geoelectric parameters, quantitative and qualitative interpretations of the data were made. The results obtained showed that: about four to five geoelectric layers have been delimited in the study area with a dominance of the KH curve, which can be used as a reference for future studies. The first two layers constitute an association of clay and laterite with resistivity values ranging from 58 to 9122 $\Omega \cdot m$ and whose thickness is between 0.6 and 13.4 m. The third layer is a potentially aquiferous laterite composed of clay, laterite and especially clay sand and cracked/good granite, with a dominance of sandy alteration whose resistivity values are between 81 and 960 $\Omega \cdot m$ and its thickness between 12.2 and 26.8 m. The fourth and fifth layers are made up of cracked/good granite with a resistivity ranging from 12 - 10705 $\Omega \cdot m$ with an average value of 1817 $\Omega \cdot m$. This study also shows that the North-East, South-West and South sectors could be the groundwater convergence zones and that the average depth of the basement aquifer roof is about 28.3 m. The geoelectric sections of certain demarcated vertical electrical sounding stations are consistent with the geologic description of the area.

Keywords

Adamawa Plateau Region, Vertical Electrical Sounding, Geoelectric Sections, Aquifer, Groundwater
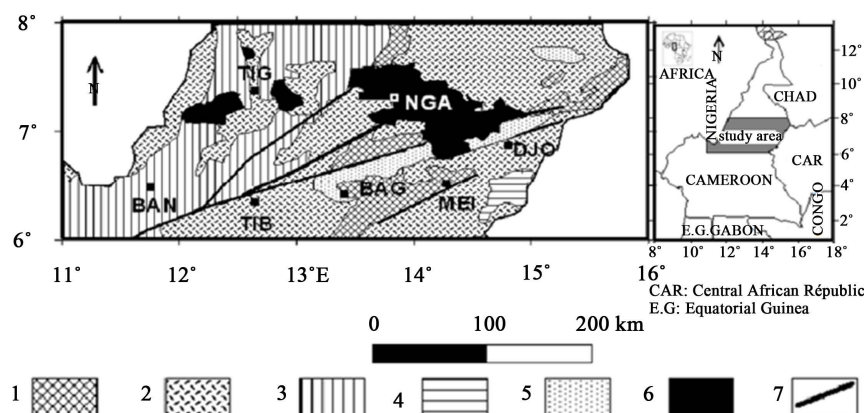
1. Introduction

1.1. Study Context

The Adamawa Plateau, located in the Adamawa region which is one of the ten regions of Cameroon, is considered as the water tower of the country. Despite this appellation, many people lack drinking water especially in rural areas where the search for sources of reliable drinking water has become an important issue for villages in this region of Cameroon. In fact, the population growth has led to a serious shortage of drinking water, which is why the drinking water points must be exploited with the greatest care in order to avoid their exhaustion and their sustainable use. This poses a great challenge for citizens and the government [1], who has to deal with the inadequate supply of drinking water in the region, which has become a chronic problem. In addition to the high population growth, the shortage of drinking water due to insufficient knowledge of the potential of the underground aquifer especially with respect to the characteristics of the latter, and the aggressive use of water [2], it is also important to pay attention to the quality of the water used [3]. It is therefore very necessary to first highlight the existence of these aquifers and their hydrogeological characteristics. As a result, the integration of aquifer parameters calculated from existing drill locations and surface resistivity parameters extracted from surface electrical measurements shall be used effectively. This work, which is an application of the geoelectric prospecting method, attempts to provide a solution to the above-mentioned problem with the aim of producing a database that could be used for detailed groundwater exploration activities in the study area.

1.2. Hydrogeological and Geologic Settings

The Adamawa plateau which is the study area of this work is found in the Adamawa region of Cameroon, which is located in the heart of Central Africa between latitudes 6°N and 8°N and Longitudes 11°E and 16°E. The vegetation encountered is of shrub savanna type with the preponderance of cereal crops. Climate changes in this region where the average temperature (between 21°C and 29°C) increases; average annual rainfall (800 mm to 1600 mm) decreases and groundwater has increased up to 4 m in 15 years [4]. Geologically, the Adamawa plateau region of Cameroon (**Figure 1**) presents itself as a volcanic axis characterized by a fissured basaltic volcanism. The fault leaving Foumban, joins it and crosses away almost diagonal. It is one of the zones in Cameroon where one can meet several geological accidents.

The basement of the Adamawa plateau region consists of a Precambrian granito-gneiss complex (**Figure 1**) that recorded Pan-African granitization [6]. That basement is overlain by a sequence of basaltic to andesitic lavas that are largely of Tertiary age [7]. These lavas are essentially alkaline indicating an affinity to continental rifts [8]. The sedimentary formations here are mainly composed of conglomerates and marl of the Cretaceous Mbere and Djerem Troughs [7] [9]. These formations have undergone intense tectonic activity resulting in the emplacement

Figure 1. Geologic map of study area (modified from [5]). 1: High grade metamorphosed paleoproterozoic gneiss; 2: Syn-tectonic panafrican granite; 3: principal undifferentiated panafrican Gneiss; 4: panafrican Metasediments; 5: envelope of cretaceous sediments; 6: cenozoic Volcanism; 7: Central Cameroon fault line.

of basin structures which were frequently filled by volcanic material upwelling through deep fractures in the Adamawa region.

The Adamawa plateau is sometimes called the "water tower" of Cameroon, since a large number of rivers of the country have their sources in this region and experience floods from May to September during the rainy season. The rivers of the region flow into three different basins: the Niger River, Lake Chad, and the Atlantic Ocean. The hydrogeology of the region is marked by continuous alterite aquifers. In the granito-gneisses, this reservoir is generally from 1 to 20 m where it is characterized by clay dominance [10]. These aquifers overcome a cracked horizon of the granite-Gneissic basement fed by rainwater and stream beds. It constitutes the aquifer that is essentially prospecting because it concentrates most of the groundwater reserves and is supposed to be protected from seasonal fluctuations [11]. We can note the presence of wells and boreholes that are functional all year round, resulting from multiple development support programs.

1.3. Recent Geophysical Works and Problem Statement

The Adamawa plateau has also been the subject of a recent study that portrays the study of the hydrogeophysical characteristics of the Pan-African aquifer [12]. This study establishes unequal distribution of transmissivities by an alternative approach based on the interpretation of vertical electrical sounding data. Another study based on electrical resistivity tomography (ERT) and self-potential data was carried out at Meiganga in the Department of Mbere, in the Adamawa region [13]. This made it possible to delimit the groundwater producing areas in this locality and the resistivities of the geological formations encountered. However, these studies do not show a geophysical mapping of the aquifer and a station-by-station geoelectric study in various localities in the region. The types of data used in these studies do not make it possible to sufficiently assess the cha-

racteristics of aquifer zones throughout the region. All these aforementioned raise the need to carry out a geophysical study using a more direct method of all vertical electrical soundings conducted in the region.
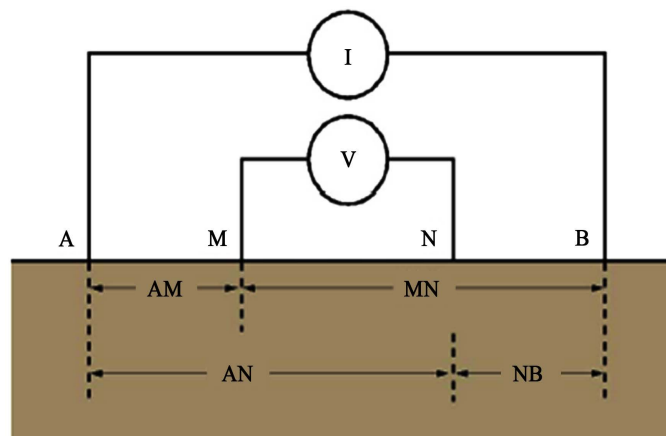
2. Data Acquisition and Methodology

2.1. Data Acquisition

The Schlumberger configuration of a linear electrodes array (AMNB) was used to locate and characterize aquifers. With this technique, whereby electrical resistivity variations are expressed as a function of depth, forty (40) Vertical Electrical Sounding (VES) have been carried out in the study area using the terrameter model SAS-300B. The operational principle rests on the fact that ground injection of current through current electrodes A and B enables the measurement of the potential drop between potential probes M and N (**Figure 2**). Potential electrodes M and N are kept fixed at the center of the array while current electrodes A and B are moved outward symmetrically [14]. By increasing the distance between the current electrodes from 3 to 166 m, the layer resistance ΔV/I was directly measured, and its apparent resistivity ρ_a was calculated using Ohm's law (Equation (1)) while taking Equation (2) into consideration. Apparent resistivity depends on several factors such as true layer resistivities, their boundary, and the location of electrodes. However, lack of uniformity or split of layers can be observed.

$$\rho_a = K \frac{V_{MN}}{I_{AB}} \tag{1}$$

- K (in m) is the geometric factor depending on the array of electrodes;
- V_{MN}: potential drop between electrodes M and N, in mV;
- I_{AB}: electric current injected between electrodes A and B, in mA. Where:

$$K = \frac{2\pi}{\left(\dfrac{1}{AM} - \dfrac{1}{BM} - \dfrac{1}{AN} + \dfrac{1}{BN} \right)} \tag{2}$$

Figure 2. Principle of implementation of the geoelectrical method.
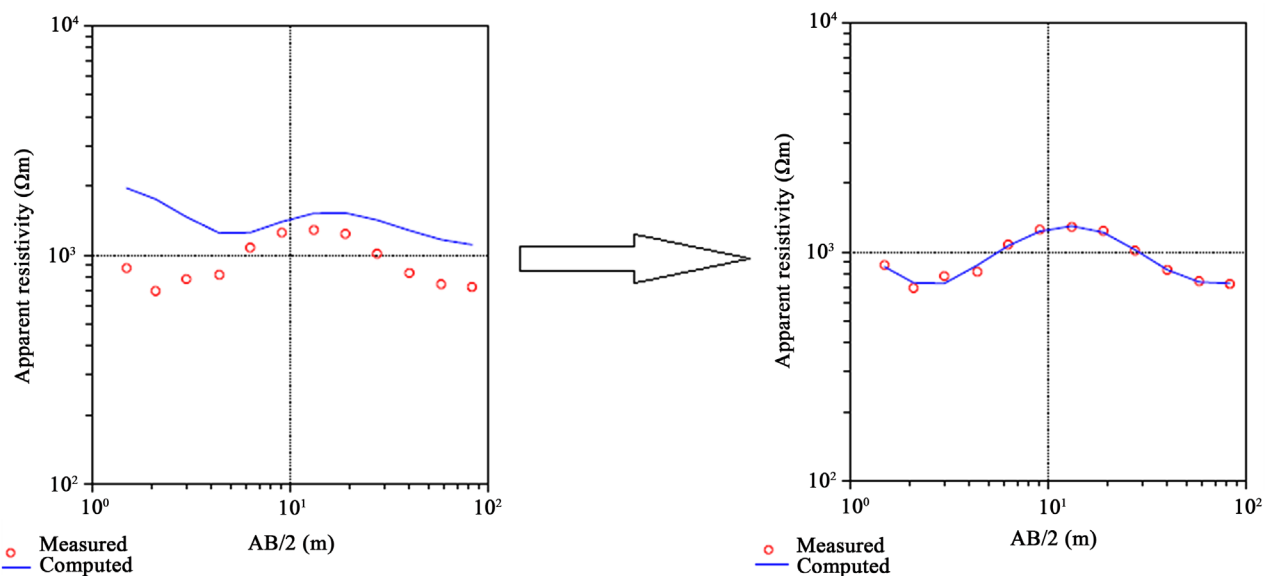
2.2. Methodology

The curve-matching technique was used in this study to calibrate and interpret the sounding curves [15]. Calibration was conducted with experimental boreholes drilled in the vicinity of several VES points. These experimental parameters were thereafter accurately interpreted using an inverse technique program [16] [17]. In this case, a weighted least squares inversion algorithm was used to propose geoelectrical models of the study area. The process here is done in several steps which include:

a) Importing survey data collected in the field

On the sample sheet used during the data collection, two variables were used for the modeling: the values of the spacings of AB/2 and that of apparent resistivity ρ_a. Thus using the modeling tool JOINTEM (joint interpretation of electromagnetic and geoelectrical soundings using 1-D layered earth model), more precisely in the box denoted "method by direct current", abilogarithmic paper is employed whose abscissa takes the values of AB/2 and its ordinate takes values of ρ_a.

b) Matching curves

The inversion process involves bringing the theoretical curve so that it superimposes itself the most possible on the points of soundings. This curve has well defined parameters which are the number of layers, the resistivity of layers and the thickness or depth of the layers (**Figure 3**). However the overlaying of the curves can be correct but the parameters obtained do not reflect the reality, and so there will be need to change these parameters from the information available at first sight. This is in order to obtain a quadratic error average (RMS) value as small as possible and the sum of damping factors equal to one. This process was carried out taking into account several precautions, such as the precision of various

Figure 3. Principle of least squares inversion of vertical electrical sounding data (this figure illustrates the superposition of the computed curve in blue on the points of measurement in red).

calculations, a reasonable geologic concept and the hypothesis of a one-dimensional (1D) medium [18]. The geologic conditions of the region were favorable for assuming 1D model for vertical electrical soundings data interpretation [12].

3. Results and Discussion

3.1. Results

The results of this study are from a quantitative study done with vertical electrical sounding curves summarized in a table and from a qualitative study through cartography.

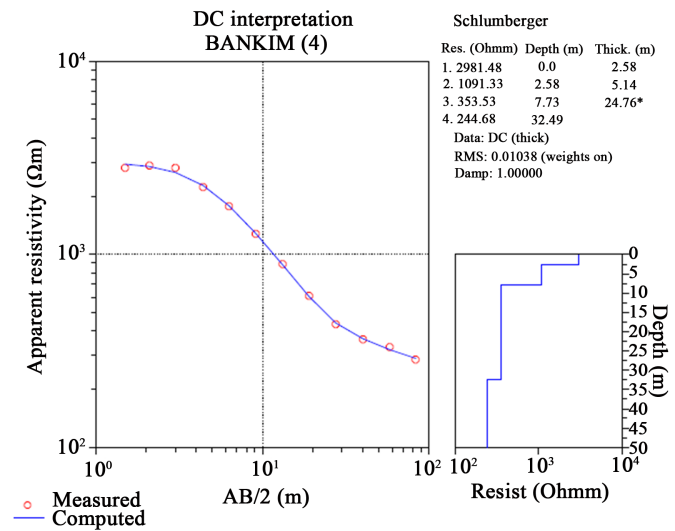#### 3.1.1. Geoelectrical Survey Curves

In the study area, forty (40) vertical electrical soundings were performed and interpreted. Their interpretation made it possible to propose a geoelectrical succession that is as close as possible to the geophysical measurements made in the field (Figure 2). Several types of curves have also been identified. In addition, the presence of some drilling logs in the area made it possible to draw a geoelectrical section of the subsoil of the area (Figure 4) which highlights the presence of topsoil, laterite, lateritic clay, clayey sand and granite described by Figure 5. The interpretations of these curves are regrouped in Table 1.

The curves obtained in this study, as presented on Table 1, are of AA, AK, HA, KH, KQ, QH and QQ types for the four (04) layer terrain models and HKH, KHA and KQH for the five (05) layer terrain models. The most representative curves are of type KH with a rate of 22.5%. The dominance of these curve types shows a homogenous subsurface succession, and, in most sounding curves the same layers were found.
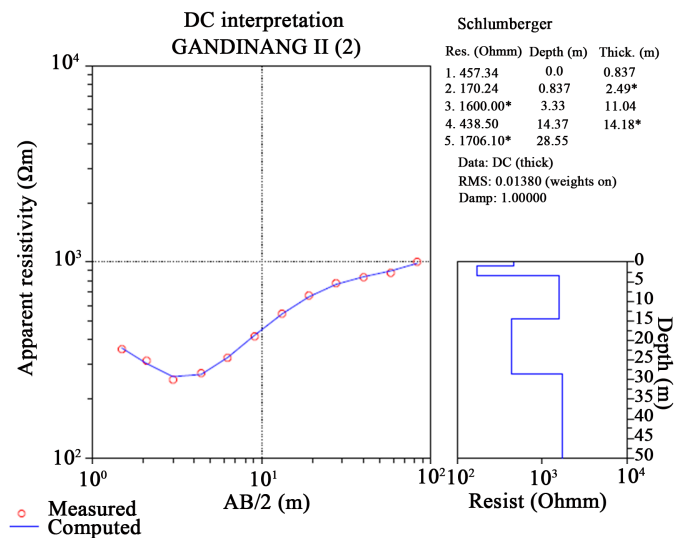
Close to the surface, a dominance of the laterite and sometimes associated with the clay was obtained whose resistivity varies between 457 - 9122 $\Omega \cdot m$ and the thickness between 0.6 - 6.5 m. There is also the presence of topsoil at stations S.1, S.2, S.9, S.10, S.17, S.18, S.21 and S.36 with a resistivity varying from 61 - 381 $\Omega \cdot m$ and the thickness between 0.2 - 3.2 m.

The second layer, more or less weathered, is a clay-laterite complex dominated by clay. Its resistivity varies between 58 - 4828 $\Omega \cdot m$ and the thickness between 1.3 - 13.4 m. At stations S.12, S.31 and S.32, the lithology makes it possible to deduce a very resistant granite upwelling with a resistivity range of 5822 - 15,000 $\Omega \cdot m$ and thickness range of 3.3 - 5.3 m. This second layer contributes to the development of groundwater because it allows the infiltration of surface water to the cracked medium of the basement.

The third and fourth layers have been identified as potential aquifer zones. The third layer is dominated by clayey sand with a resistivity range of 81 - 960 $\Omega \cdot m$ and thickness of 12.2 - 26.8 m. Using lithology, an alteration was highlighted which is clay at stations S.1, S.9 and S.36 with resistivity ranging from 42 - 69 $\Omega \cdot m$ and thickness of 6.4 - 12.1 m. Laterite was also found at stations S.7, S.8, S.15, S.22 and S.26 with a resistivity of 1251 - 2669 $\Omega \cdot m$ and thickness

DC interpretation
BANKIM (4)

Schlumberger

Res. (Ohmm)	Depth (m)	Thick. (m)
1. 2981.48	0.0	2.58
2. 1091.33	2.58	5.14
3. 353.53	7.73	24.76*
4. 244.68	32.49	

Data: DC (thick)
RMS: 0.01038 (weights on)
Damp: 1.00000

Apparent resistivity (Ωm) — AB/2 (m) — Resist (Ohmm) — Depth (m)

○ Measured
— Computed

(a)

DC interpretation
GANDINANG II (2)

Schlumberger

Res. (Ohmm)	Depth (m)	Thick. (m)
1. 457.34	0.0	0.837
2. 170.24	0.837	2.49*
3. 1600.00*	3.33	11.04
4. 438.50	14.37	14.18*
5. 1706.10*	28.55	

Data: DC (thick)
RMS: 0.01380 (weights on)
Damp: 1.00000

Apparent resistivity (Ωm) — AB/2 (m) — Resist (Ohmm) — Depth (m)

○ Measured
— Computed

(b)

DC interpretation
SELAL DJERTOU (1)

Schlumberger

Res. (Ohmm)	Depth (m)	Thick. (m)
1. 1041.43	0.0	0.684
2. 2471.13	0.684	10.75
3. 374.81	11.43	24.87
4. 16.49*	36.31	

Data: DC (thick)
RMS: 0.00886 (weights on)
Damp: 1.00000

Apparent resistivity (Ωm) — AB/2 (m) — Resist (Ohmm) — Depth (m)
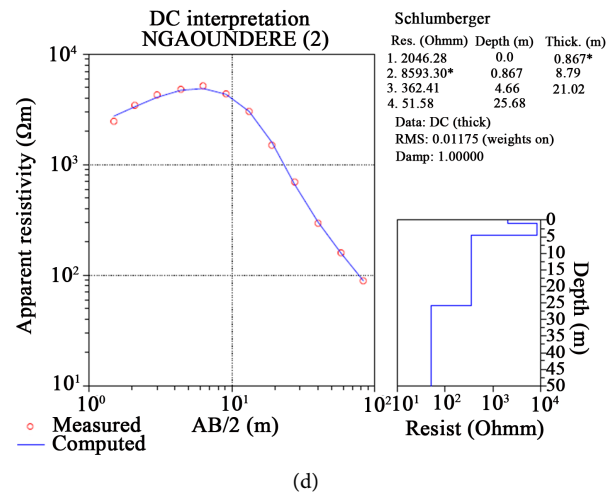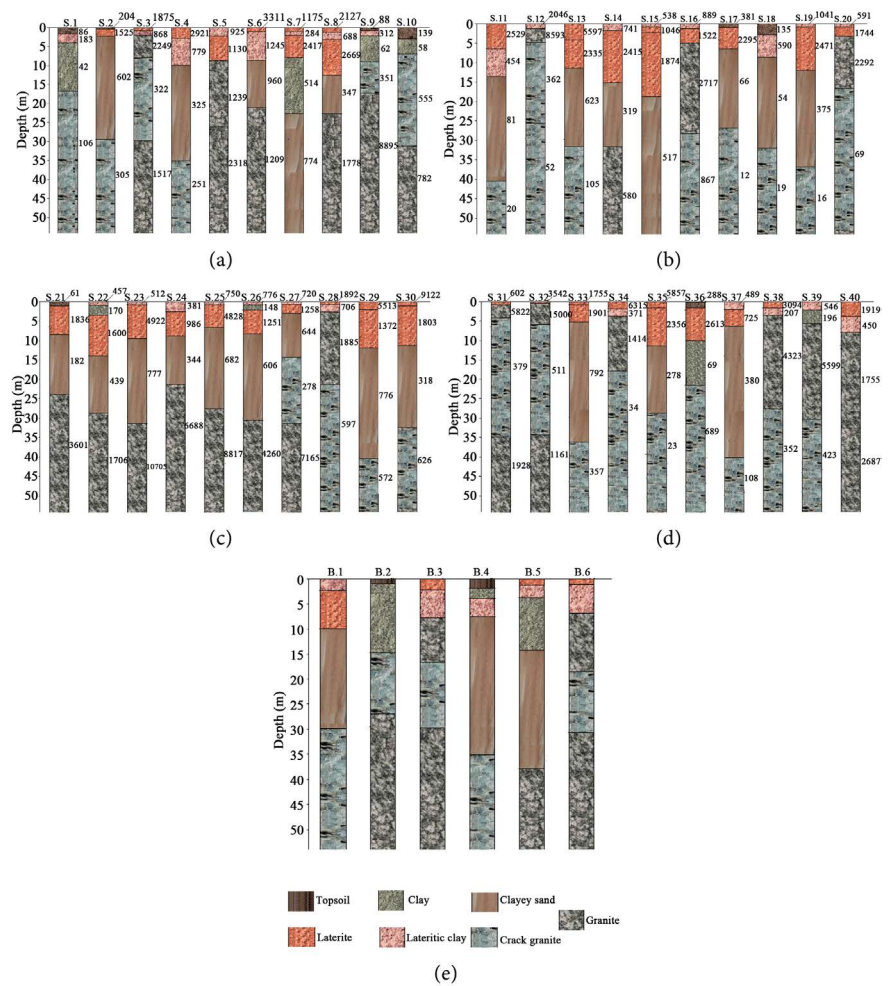
○ Measured
— Computed

(c)

(d)

Figure 4. (a): The computer interpretation curve of S.4; (b): The computer interpretation curve of S.22; (c): The computer interpretation curve of S.19; (d): The computer interpretation curve of S.12.

Figure 5. (a): Geoelectrical cuts from S1 to S10; (b): Geoelectrical cuts from S.11 to S.20; (c): Geoelectric cuts from S.21 to S.30; (d): Geoelectric cuts from S.31 to S.40; (e): Drill cuts in some localities in the study area.

Table 1. Resistivity sounding results.

Stations	Resistivity $\rho_1/\rho_2/\ldots/\rho_n$	Thickness $h_1/h_2/\ldots/h_{n-1}$	Total thickness	Lithology	Curve type
S.1: Bankim (1)	86/183/42/106	2/2.5/12.1	16.6	Topsoil/Lateritic Clay/Clay/Cracked Granite	KH
S.2: Bankim (2)	204/1525/602/305	0.2/2.5/26.8	29.5	Topsoil/laterite/Clay sand/Cracked Granite	KQ
S.3: Bankim (3)	1875/868/2249/322/1517	0.7/1.2/6/22	30	laterite/Lateritic Clay/Granite/Cracked Granite/Granite	HKH
S.4: Bankim (4)	2921/779/325/251	3.1/7/25.2	35.2	Laterite/Lateritic Clay/Clayey sand/Cracked Granite	QQ
S.5: Bankim (5)	925/1130/1239/2318	2.5/6.3/17.9	26.7	Lateritic clay/Laterite/Granite/Granite	AA
S.6: Bankim (6)	3311/1245/960/1209	1/7.7/12.3	21	Laterite/Lateritic Clay/Clayey sand/Granite	QH
S.7 Meidougou (1)	1175/284/2417/514/774	0.8/0.8/6/15	22.6	Laterite/Lateritic Clay/Laterite/Clay/Clayey Sand	HKH
S.8 Meidougou (2)	2127/688/2669/347/1778	1.4/2.1/9/10	22.5	Laterite/Lateritic Clay/Laterite/Clayey Sand/Granite	HKH
S.9: Banyo (1)	88/312/62/351/8895	0.6/1.7/6.4/8.4	17	Topsoil/Laterite Clay/Clay/Cracked Granite/Granite	KHA
S.10 Banyo (2)	139/58/555/7826	3.2/4/23.9	31.1	Topsoil/Clay/Cracked Granite/Granite	HA
S.11 Ngaoundéré (1)	2529/454/81/20	6.5/7.1/26.8	40.4	Laterite/Lateritic Clay/Clayey Sand/Cracked Granite	QQ
S.12 Ngaoundéré (2)	2046/8593/362/52	0.9/3.8/21	25.7	Laterite/Granite/Cracked Granite/Cracked Granite	KQ
S.13 Ngaoundéré (3)	5597/2335/623/105	4.2/6.9/20.3	31.4	Laterite/Laterite/Clayey Sand/Cracked Granite	QQ
S.14 Ngaoundéré (4)	741/2415/319/580	1.7/13.4/16.3	31.4	Lateritic clay/Laterite/Clayey Sand/Granite	KH
S.15 Ngaoundéré (5)	538/1046/1874/517	0.6/1.7/16.5	18.8	Lateritic Clay/Laterite/Laterite/Clayey Sand	AK
S.16 Kaka	889/1522/2717/867	1.2/3.8/23	28	Lateritic clay/Laterite/Granite/Cracked Granite	AK
S.17 Leswoka (1)	381/2295/66/12	0.9/5/21	26.9	Topsoil/laterite/Clayey sand/Cracked Granite	KQ
S.18 Leswoka (2)	135/590/54/19	2.5/6.4/22.8	31.7	Topsoil/Laterite Clay/Clayey Sand/Cracked Granite	KQ
S.19 Selal Djertou (1)	1041/2471/375/16	0.7/10.8/24.9	36.4	Lateritic clay/Laterite/Clayey Sand/Cracked Granite	KQ
S.20 Selal Djertou (2)	591/1744/2292/69	0.7/2.4/13.2	16.3	Lateritic clay/Laterite/Granite/Cracked Granite	AK

Continued

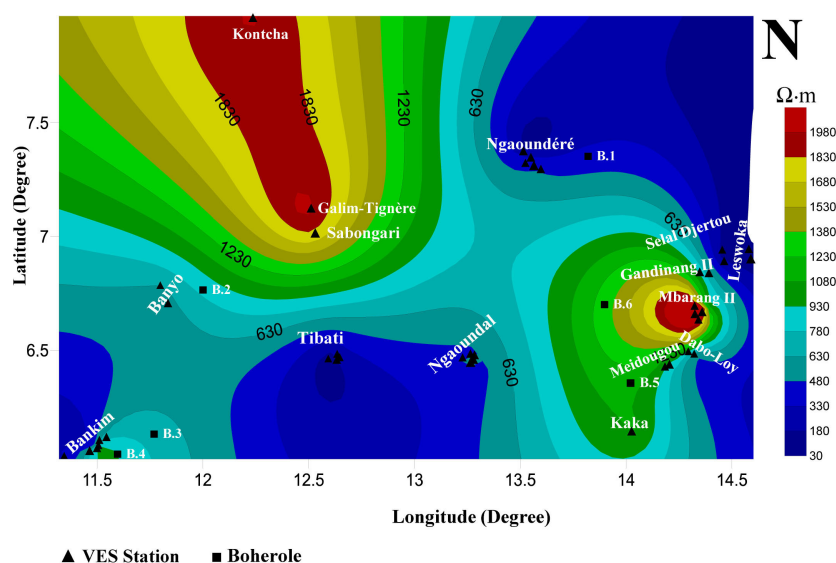|					
S.21 Gandinang (1)	61/1836/182/3601	1.1/7.5/15.4	24	Topsoil/laterite/Clayey sand/Granite	KH
S.22 Gandinang (2)	457/170/1600/439/1706	0.9/2.5/11/14.2	28.6	Lateritic Clay/Clay/Laterite/Clayey sand/granite	HKH
S.23 MbarangII (1)	512/4922/777/10705	0.7/8.7/21.3	30.7	Lateritic Clay/Laterite/Clayey Sand/Granite	KH
S.24 Mbarang II (2)	381/986/344/6688	2.3/6.6/12.2	21.1	Lateritic clay/Laterite/Clayey Sand/Granite	KH
S.25 Mbarang II (3)	750/4828/682/8817	0.6/6.2/20.8	27.6	Lateritic clay/Laterite/Clayey Sand/Granite	KH
S.26 Mbarang II (4)	776/148/1251/606/4260	0.7/1.3/6.1/22.7	30.8	Lateritic Clay/Clay/Laterite/Clayey Sand/Granite	HKH
S.27 Dabo-loy (1)	720/1258/644/278/7165	0.6/2.1/11.9/16.8	31.4	Lateritic clay/Laterite/Clayey Sand/Cracked Granite/Granite	KQH
S.28 Dabo-loy (2)	1892/706/1885/597	0.6/1.8/18.9	21.3	Laterite/Lateritic Clay/Granite/Cracked Granite	HK
S.29 Ngaoundal (1)	5513/1372/776/572	2/10.2/28	40.2	Laterite/laterite/Clayey sand/Cracked Granite	QQ
S.30 Ngaoundal (2)	9122/1803/318/626	0.9/9.8/21.8	32.5	Laterite/laterite/Clayey sand/Cracked Granite	QH
S.31 Ngaoundal (3)	602/5822/379/1928	0.8/3.3/30.7	34.8	Laterite/Granite/Cracked Granite/Granite	KH
S.32 Ngaoundal (4)	3542/15000/511/1161	0.4/5.3/28.6	34.3	Laterite/Granite/Cracked Granite/Granite	KH
S.33 Ngaoundal (5)	1755/1901/792/357	0.9/4.6/30.6	36.1	Laterite/Laterite/Clayey Sand/Cracked Granite	KQ
S.34 Tibati (1)	6315/371/1414/34	1.6/1.8/14.2	17.6	Laterite/Lateritic Clay/Granite/Cracked Granite	HK
S.35 Tibati (2)	5857/2356/278/23	1.3/11.2/16.4	28.9	Laterite/Laterite/Clayey Sand/Cracked Granite	QQ
S.36 Tibati(3)	288/2613/69/689	1.3/8.7/11.9	21.9	Topsoil/Laterite/Clay/Cracked Granite	KH
S.37 Tibati (4)	489/725/380/108	2.1/4.1/33.8	40	Lateritic clay/Laterite/Clayey Sand/Cracked Granite	KQ
S.38 Kontcha	3094/207/4323/352	1.5/2/23.8	27.3	Laterite/Lateritic clay/Granite/Cracked Granite	HK
S.39 Sabongari	546/196/5599/423	2/3/25.2	30.2	Lateritic clay/Clay/Granite/Cracked Granite	HK
S.40 Galim-Tignère	1919/450/1755/2687	3.5/3.9/25.2	32.6	Laterite/Lateritic clay/Granite/Granite	HK

between 6 - 16.5 Ω·m. Finally, the presence of the cracked/good granitic basement was noticed at stations S.3, S.5, S.10, S.12, S.16, S20, S.28, S.31, S.32, S.34, S.38, S.39 and S.40 whose resistivity varies between 362 - 5599 Ω·m and the thickness between 6 - 30.7 m. The fourth layer is relatively current-conducting and dominated by weathered granite whose resistivity varies between 278 - 351 Ω·m and the thickness between 8.4 - 22 m; and also by clayey sand with a resistivity range of 347 - 606 Ω·m and thickness between 10 - 22.7 m.

The fourth and fifth layers would be good/cracked granitic basement with a resistivity ranging from 12 - 10,705 Ω·m. Fracturing is intense at stations S.1, S.11, S.12, S.13, S.17, S18, S19, S20, S.34, S.35 and S.37; with a resistivity range of 16 - 108 Ω·m or an average of 47 Ω·m and an infinite thickness, because they form the last layer and could constitute a good confined aquifer. This strong resistivity contrast found in the basement zone is due to the fact that the resistivity of the rocks depends on several factors such as the content of interstitial fluids, weathering and fracturing [19].

Resistivity measurements separate the subsurface into different layers based on their resistivity values. Litho-log data was obtained from borehole data from the study area. These litho-logs were compared with the geoelectric sections for areas close to borehole points. The correlation was based on the fact that a litho-log differs from a geoelectric log when the boundaries of the litho-log do not coincide with the boundaries of different resistivity.

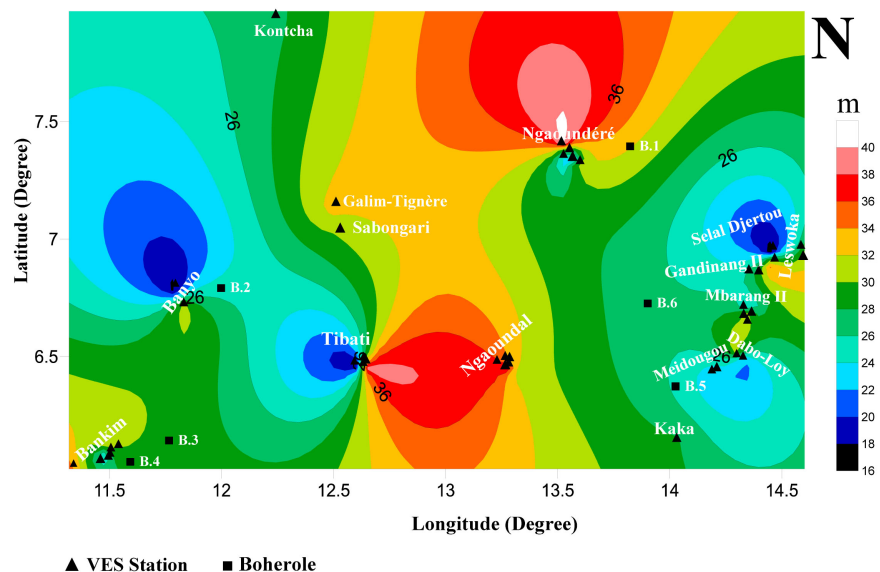### 3.1.2. Iso-Resistivity and Iso-Depth Maps of the Aquifer Roof

The aim of the iso-resistivity map is to obtain a visual representation of the apparent resistivity of the zones where the vertical electrical soundings were carried out. A proposal is presented here as an example of a reconstruction corresponding to the map of apparent resistivities for the value AB/2 = 83 m as shown in Figure 6.

Figure 6. Iso-resistivity map of the aquifer in the study area.

The apparent resistivity ranges from less than 30 Ω·m to more than 1980 Ω·m with the North-East, South-West and South sectors particularly conducive (ρ_a < 330 Ω·m). These could be the areas of convergence of groundwater through cracked granite. On the other hand, the North-West and East sectors are very resistant (ρ_a > 1980 Ω·m) which would be healthy granite.

The iso-depth map of the aquifers (**Figure 7**) shows that, the depth varies between 16 m and more than 40 m, with an average of 28.3 m. This depth would actually be that of rock where we can have cracked zones, because the hydrogeological investigations is based on the search for the zones of cracking of the base which have in general a very good permeability [20]. From a hydraulic point of view, it is the depth from which the first arrivals of water are very likely. However, we note that zones with high aquifer potential have depths greater than 28 m.

▲ VES Station   ■ Boherole

Figure 7. Depth to the top of aquifer in the area.

3.2. Discussions

The interpretation of the vertical electrical soundings made it possible to highlight the geoelectrical models of the basement of the study area. To this end, the subsoil of the study area has been subdivided into three major groups. The first is a shallow (<14 m) superficial infiltration zone dominated by laterite whose resistivity is quite high (>1000 Ω·m) and clay (<600 Ω·m). The second zone is a weathered zone which, in the majority of cases constitutes a superficial aquifer with a resistivity range between 81 Ω·m and 960 Ω·m and thickness range between 12.2 m and 26.8 m. This weathered zone overcomes a granitic horizon that presents a large variety of resistivity range (between 12 Ω·m and 10705 Ω·m) thus highlighting the strong heterogeneity of rock. The deep water producing areas would be around 16 m and 40 m of depth. However it could be noted that the results obtained by tomographic and Self-Potential data analysis in part of

the region of Meiganga (Meying *et al.*, 2018) revealed the presence of lateritic formations (lateritic soils, laterites) with high resistivity values (>2000 Ohm·m), a gneissic weathered/fractured arena with low resistivity values (<850 Ohm·m) which represents the aquifer training and the gneissic basement. As a result, the inverted resistivity models have revealed productive groundwater zones at depths of 20 to 25 m and are considered to be deeper groundwater zones with depths of about 10 to 13 m, for shallow groundwater [13]. However, some differences are observed when the results are compared, this may be due to the greater investigation area which is more extensive in the case of our study but also the type of data exploited.

In addition, a comparative study between the geophysical parameters obtained in the most recent study by inverse slope method [12] and those obtained by the least-squares inversion has been carried out and shows by Table 2.

This table shows that the parameters of the aquifer are almost similar with both approaches. Therefore, the results obtained are in agreement with those of Arétouyap *et al.* (2018).

Table 2. Comparison of the results from studies using two approaches in the area of study.

Method	Geophysical parameters
Inverse slope method	For the first set, aquifer resistivity varies between 212 and 640 Ω·m and its thickness between 20 and 30 m. For the second trend, the aquifer resistivity ranges from 111 to 962 Ω·m and the thickness from 10 to 30 m.
Least-squares inversion	The weathering aquifer has a resistivity that varies between 81 and 960 Ω·m and the thickness between 12.2 and 28.6 m. The average resistivity of the deep aquifer is 1817 Ω·m.

Alteration is an important factor in the search for groundwater, because the weathered layers are very porous and weakly permeable due to the presence of clay. Weathered layers are known to have a very good water storage function [21]. The stations of great hydrogeological interest are S.2, S.4, S.11, S.13, S.17, S18, S.19, S.23, S.25, S.26, S.29, S.30, S.33 and S.37 because they have weathered and fractured formations of great thicknesses On the other hand, the weathered layers are weak thicknesses and almost non-existent in some stations like S.3, S.12, S.16, S20, S.28, S.31, S.32, S.38, S.39 and S.40.

The interpretation carried out on vertical electrical sounding curves corroborate with lithological data from boreholes in the area.

4. Conclusion

Forty (40) vertical electrical soundings were exploited by the least-squares inversion method to characterize the aquifers in the Adamawa Plateau region of Cameroon. This study shows that: 1) the geological layers identified in this zone are made up of: top soil, laterite, clay, clay sand and granite whose resistivities have been determined; 2) Several types of curves have been identified: AA, AK, HA, KH, KQ, QH and QQ for the four (04) layer models and HKH, KHA and KQH

corresponding to five (05) layer terrain models; 3) The sectors that could well be groundwater convergence zones are located to the North-East, South-West and South of the Adamawa plateau; 4) The roof of the basement aquifer varies between 16 m and 40 m, an average of 28.3 m. Cracked aquifers are less sensitive to pollution, unlike aquifers of laterites. However, in most cases, the laterites more crack horizon constitutes a composite aquifer that functions as a whole, especially when it is exploited by deep drilling. Hence, there is the need to focus on the thickness of the weathered layer and the conductive character of the underlying layer which is the cracked horizon. However, the thickness of the granite layer may not be fully evaluated at very great depth through this work. It nonetheless provides an overview of shallow subsurface aquifer systems and delineates areas for the groundwater development programs in the region.

Acknowledgements

Conflicts of Interest

The authors declare no conflicts of interest regarding the publication of this paper.

References

[1] Teikeu, A.W., Njandjock, N.P., Ndougsa, M.T. and Tabod, T.C. (2012) Geoelectric Investigation for Groundwater Exploration in Yaounde Area, Cameroon. *International Journal of Geosciences*, **3**, 640-649. https://doi.org/10.4236/ijg.2012.33064

[2] Enyegue, A.N.F.M., Ndougsa, M.T., Njandjock, N.P., Assembe, S. and Manguelle, D.E. (2014) Groundwater Exploration Using Geoelectrical Investigation in Bafia Area, Cameroon *Journal of Earth Sciences and Geotechnical Engineering*, **4**, 61-75.

[3] Aretouyap, Z., Njandjock, N.P., Ekoro, H.N., Meli, L.J. and Lépatio, A.T. (2014) Investigation of Groundwater Quality Control in Adamaoua-Cameroon Region. *Journal of Applied Sciences*, **14**, 2309-2319.

[4] Aretouyap, Z., Njandjock, N.P., Bisso, D., Nouayou, R., Lengue, B. and Lépatio, A.T. (2014) Climate Variability and Its Possible with Water Resources in Central Africa. *Journal of Applied Sciences*, **14**, 2219-2233.

[5] Ngnotue, T., Nzenti, J.P., Barbey, P. and Tchoua, F.M. (2000) The Ntui-Betamba High Grade Gneisses in Cameroon. *Journal of African Earth Sciences*, **31**, 369-381. https://doi.org/10.1016/S0899-5362(00)00094-4

[6] Dumont, J.F. (1987) Etude structurale des bordures Nord et Sud du plateau de l'Adamaoua: Influence du contexte atlantique. *Géodynamique*, **2**, 55-68.

[7] Le Maréchal, A. and Vincent, R.P. (1971) Le fossé crétacé du Sud Adamaoua (Cameroun). *Cahier O.R.S.T.O.M., sér. Géol.*, **3**, 67-83.

[8] Kampunzu, B.A., Caron, H.J. and Lubala, T.R. (1986) The East African Rift, Magma Genesis and Astheno-Lithospheric Dynamism. *Episodes*, **9**, 211-216. https://doi.org/10.18814/epiiugs/1986/v9i4/002

[9]   Lasserre, M. (1961) Étude géologique de la partie orientale de l'Adamaoua (Cameroun Central) et les principales sources minéralisées de l'Adamaoua. *Bull. Dir. Mines et Géologie du Cameroun*, No. 4, 130 p.

[10]   Djeuda, T.B.H., Tanawa, E., Temgoua, E., Siakeu, J. and Ngo, M.B. (1999) Modèle de circulation, mécanisme de recharge et temps relatif de séjour des eaux des nappes souterraines des altérites en milieu cristallin: Cas du bassin versant de l'Anga'a, Yaoundé-Cameroun. Collect. Géocam, 2/1999, Ed. Press. Univ. de Yaoundé, Yaoundé, 117-126.

[11]   Gnamba, M.F., Oga, Y.S.M., Gnagne, T., Lasm, T. and Beimi, J. (2014) Analyse de la productivité des aquifères de fissures du socle paléoprotérozoïque de la région de katiola (centre-nord de la Côte d'Ivoire). *European Scientific Journal*, **10**, 79-98.

[12]   Aretouyap, Z., Bisso, D., Njandjock, N.P., Amougou, M.L.E. and Asfahani, J. (2018) Hydrogeophysical Characteristics of Pan-African Aquifer Specified through an Alternative Approach Based on the Interpretation of Vertical Electrical Sounding Data in the Adamawa Region, Central Africa. *Natural Resources Research*, **28**, 63-77. https://doi.org/10.1007/s11053-018-9373-8

[13]   Meying, A., Bidichael, W.W.E., Gouet, D., Ndougsa, M.T., Kuiate, K. and Ngoh, J.D. (2018) Hydrogeophysical Investigation for Groundwater Resources from Electrical Resistivity Tomography and Self-Potential Data in the Méiganga Area, Adamawa, Cameroon. *Hindawi International Journal of Geophysics*, **2018**, Article ID: 2697585. https://doi.org/10.1155/2018/2697585

[14]   Telford, W.M., Geldart, L.P. and Sheriff, R.E. (1990) Applied Geophysics. Cambridge University Press, Cambridge, 870 p. https://doi.org/10.1017/CBO9781139167932

[15]   Orellana, E. and Mooney, H.M. (1966) Master Tables and Curves for Vertical Electrical Sounding over Layered Structures. Interciencia, Madrid.

[16]   Zohdy, R.A.A. (1989) A New Method for the Automatic Interpretation of Schlumberger and Wenner Sounding Curves. *Geophysics*, **54**, 245-253. https://doi.org/10.1190/1.1442648

[17]   Zohdy, R.A.A. and Bisdorf, R.J. (1989) Schlumberger Sounding Data Processing and Interpretation Program. US Geological Survey, Washington DC.

[18]   Dey, H. and Morrison, H. (1979) Resistivity Modeling for Arbitrarily Shaped 3-D Structures. *Geophysics*, **44**, 753. https://doi.org/10.1190/1.1440975

[19]   Chapellier, D. (2001) Prospection électrique de surface. Cours Online de Géophysique. Univ. Lausanne, 34 p.

[20]   Engalenc, M., Grellot, U.C. and Lachaud, J.C. (1979) Inter-African Committee of Hydraulic Studies. Vol 2. 193 p.

[21]   CIEH (1981) Méthodes d'étude et de recherché de l'eau souterraine des roches cristallines de l'Afrique de l'Ouest. *Géohydraulique*, **38**, 100 p.